Wind and Structures, *Vol. 22, No. 3 (2016) 273-290*
DOI: http://dx.doi.org/10.12989/was.2016.22.3.273

Insight into coupled forced vibration method to identify bridge flutter derivatives

Fuyou Xu*, Xuyong Ying and Zhe Zhang

School of Civil Engineering, Dalian University of Technology, Dalian 116024, China

(Received September 10, 2014, Revised October 17, 2015, Accepted November 12, 2015)

Abstract. The flutter derivatives of bridge decks can be efficiently identified using the experimentally and/or numerically coupled forced vibration method. This paper addresses the issue of inherent requirement for adopting different frequencies of three modes in this method. The aerostatic force components and the inertia of force and moment are mathematically proved to exert no influence on identification results if the signal length (t) is integer ($n=1,2,3...$) times of the least common multiple (T) of three modal periods. It is one important contribution to flutter derivatives identification theory and engineering practice in this study. Therefore, it is unnecessary to worry about the determination accuracy of aerostatic force and inertia of force and moment. The influences of signal length, amplitude, and frequency ratio on flutter derivative are thoroughly investigated using a bridge example. If the signal length t is too short, the extraction results may be completely wrong, and particular attention should be paid to this issue. The signal length $t=nT$ ($n\geq 5$) is strongly recommended for improving parameter identification accuracy. The proposed viewpoints and conclusions are of great significance for better understanding the essences of flutter derivative identification through coupled forced vibration method.

Keywords: bridge; flutter derivative; forced vibration method; multiple-degree-of-freedom coupling; theoretical proof; exemplification

1. Introduction

Flutter derivatives of a bridge deck can be efficiently extracted using the forced vibration method based on wind tunnel tests and/or numerical simulations. Ukeguchi *et al*. (1966) proposed the forced vibration method for measuring the aeroelastic forces of bridge decks. During the 1970s to 1980s, this method was rarely employed as it requires complicated experimental setup. Falco *et al.* (1992) investigated the validity of a linear model based on forced vibration method, and the influence of wind angle of incidence on bridge aeroelastic behavior was also studied. Li (1995) conducted a forced vibration test in a water channel to measure the flutter derivatives. An advantage of using water as fluid medium is that higher accuracy can be expected due to higher density of water compared to air. Noda *et al*. (2003) inidicated the effect of vibration amplitude on flutter derivatives cannot be ignored for bridge decks with complex cross sections. Diana *et al.* (2004) presented an experimental setup with active turbulence generator to execute both forced

*Corresponding author, Associate Professor, E-mail: fuyouxu@hotmail.com

http://www.techno-press.org/?journal=was&subpage=8 ISSN: 1226-6116 (Print), 1598-6225 (Online)

and free motion tests, by which the flutter derivatives, admittance functions, and vortex-induced vibrations can be studied by changing the average position in terms of angle of incidence and yaw angle. Chen *et al*. (2005) examined the frequency and amplitude effects on flutter derivatives and the nonlinear characteristics of aerodynamic forces on bridge decks, which showed that flutter derivatives are moderately dependent on amplitude and frequency.

The references cited above are all experimental studies with 1-Degree-Of-Freedom (1-DOF) cases based on a non-coupling vibration scheme. This experimental setup is simple compared to that of coupled driven instrument. However, the coupled modes are preferred as they consume less time to extract the same amount of flutter derivatives and also provide similar accuracies. Based on the 1-DOF and coupled 2-DOF (vertical and torsion) forced vibrations, Matsumoto *et al*. (1993) investigated the influence of vibration mode on flutter derivatives. Their results indicated that flutter derivatives of a flat rectangular cross section (like a thin airfoil) are independent of vibration mode, while they are significantly influenced by the vibration mode for bluff rectangular section. Guo (2006) and Niu *et al*. (2007) presented 3-DOF coupling forced vibration setups and indicated that the identification results are more satisfactory compared to those of free vibration techniques.

To date, numerical simulations results presented in the literatures mainly focused on the 1-DOF case. Walther and Larsen (1997) developed a DVM simulation technique for extracting bridge deck flutter derivatives. Vairo (2003) presented a numerical model to quantify flutter derivatives in comparison with experimental measurements and indicated good agreement between two methods. Shirai and Ueda (2003) extracted the flutter derivatives of a parallel rectangular section and a flat box girder, for some parameters differences between the experimental and numerical results could be noticed. Recently, similar numerical studies on 1-DOF bridge deck cases were performed by others (e.g., Sun *et al*. 2009, Zhou and Ma 2010). To the authors' knowledge, Xu *et al*. (2014) is the only reference that focuses on the 2-DOF and 3-DOF coupled numerical simulations.

Based on many researchers' large amount of efforts and attempts, great progresses in both experimental tests and numerical simulations have been made for facilitating flutter derivatives extraction using coupled forced vibration method. Till now, acceptable accuracies can be achieved. Nevertheless, some obscure and/or unnoticed issues in flutter derivatives extraction procedures are still required to be clarified to further improve understanding of the whole identification process.

It is almost impossible to make $\omega_h = \omega_\alpha = \omega_p$ in coupled free vibration approach, but it can be easily achieved in coupled forced vibration method. However, all flutter derivatives cannot be simultaneously extracted with the same frequencies in coupled vibrations. The inherent reason has not been previously addressed. In smooth flows, during the forced vibration process, the experimentally collected or numerically simulated forces include both aerostatic and aeroelastic components. Customarily, the average of the directly acquired force is treated as the aerostatic component and eliminated to obtain the self-excited aeroelastic component, by which flutter derivatives can be subsequently extracted. However, this kind of consideration deserves to be discussed, especially for cases with large torsional amplitudes of asymmetric sections. Practically, the signal length has significant influence on identification accuracy of flutter derivatives, remarkable errors may be incurred if inappropriate signal length is selected, to which has not been paid much attention. Based on theoretical and practical demonstrations, this issue will be delved into and the rational pattern for signal selection will be presented.

In this paper, the inherent requirement of $\omega_h \neq \omega_\alpha \neq \omega_p$ in coupled forced vibration approach is explained. The influence of signal length, aerostatic components, and inertia force and moment

components on flutter derivatives will be theoretically elaborated. The proposed viewpoints are verified through a numerical example and an actual bridge deck. Finally, the major findings and contributions of this study are summarized.

2. Identification of flutter derivatives with coupled forced vibration method

The self-excited forces acting on a bridge deck section (Fig. 1) are classically represented as drag force (along-wind F_D, downwind), lift force (cross-wind F_L, upward) and torsional moment (pitching M_T, nose-up). They may be formulated in linear format, which is valid under the assumption that section vibrates with small amplitude in harmonic pattern without the occurrence of vortex shedding

$$F_L = \rho U^2 B(K_h H_1^* \frac{\dot{h}}{U} + K_\alpha H_2^* \frac{B\dot{\alpha}}{U} + K_\alpha{}^2 H_3^* \alpha + K_h{}^2 H_4^* \frac{h}{B} + K_p H_5^* \frac{\dot{p}}{U} + K_p{}^2 H_6^* \frac{p}{B}) \tag{1a}$$

$$F_D = \rho U^2 B(K_p P_1^* \frac{\dot{p}}{U} + K_\alpha P_2^* \frac{B\dot{\alpha}}{U} + K_\alpha{}^2 P_3^* \alpha + K_p{}^2 P_4^* \frac{p}{B} + K_h P_5^* \frac{\dot{h}}{U} + K_h{}^2 P_6^* \frac{h}{B}) \tag{1b}$$

$$M_T = \rho U^2 B^2 (K_h A_1^* \frac{\dot{h}}{U} + K_\alpha A_2^* \frac{B\dot{\alpha}}{U} + K_\alpha{}^2 A_3^* \alpha + K_h{}^2 A_4^* \frac{h}{B} + K_p A_5^* \frac{\dot{p}}{U} + K_p{}^2 A_6^* \frac{p}{B}) \tag{1c}$$

where h, α, and p are the vertical, torsional, and lateral displacements, respectively; ρ is the air density; U is the wind velocity; B is the bridge deck width; and H_i^*, P_i^*, and A_i^* $(i=1\sim6)$ are the flutter derivatives which depending on the cross-section geometry as well as the mean angle of incidence. They are functions of reduced frequency $K_{h/\alpha/p} = B\omega_{h/\alpha/p}/U$, and $\omega_{h/\alpha/p}$ are the vertical, torsional, and lateral vibration circular frequencies.

In order to simultaneously extract all 18 flutter derivatives, the 3-DOF coupled forced vibration is imposed on the rigid section through wind tunnel tests or by numerical simulation. The deck sinusoidal motions of $h(t) = h_0 \sin(\omega_h t + \varphi_h)$, $p(t) = p_0 \sin(\omega_p t + \varphi_p)$, $\alpha(t) = \alpha_0 \sin(\omega_\alpha t + \varphi_\alpha)$ are prescribed, where h_0, p_0 and α_0 are the amplitudes of the vertical, lateral, and torsional vibration displacements, and $\varphi_{h/p/\alpha}$ are the initial phase angels of three modes.

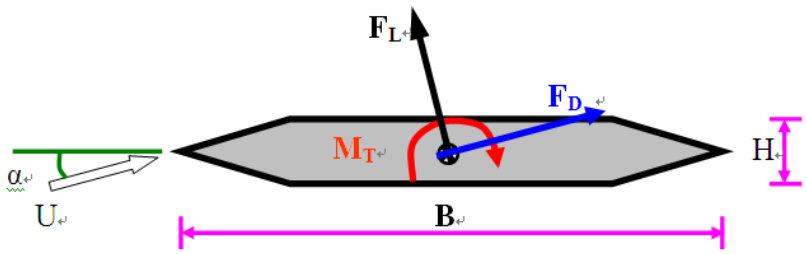

Fig. 1 Wind actions on a deck section

For the time-varying series of F_{Li}, F_{Di}, M_{Ti}, h_i, $\dot{h}_i$, p_i, $\dot{p}_i$, α_i, $\dot{\alpha}_i$, i =1, 2, 3... , Eq. (1) can be respectively rewritten as

$$F_L = \begin{pmatrix} F_{L1} & F_{L2} & \dots & F_{Ln} \end{pmatrix}^T = S_H X_H \tag{2a}$$

$$F_D = \begin{pmatrix} F_{D1} & F_{D2} & \dots & F_{Dn} \end{pmatrix}^T = S_P X_P \tag{2b}$$

$$M_T = \begin{pmatrix} M_{T1} & M_{T2} & \dots & M_{Tn} \end{pmatrix}^T = S_A X_A \tag{2c}$$

where $X_H = \begin{pmatrix} H_1^* & H_2^* & H_3^* & H_4^* & H_5^* & H_6^* \end{pmatrix}^T$,

$X_P = \begin{pmatrix} P_1^* & P_2^* & P_3^* & P_4^* & P_5^* & P_6^* \end{pmatrix}^T$,

$X_A = \begin{pmatrix} A_1^* & A_2^* & A_3^* & A_4^* & A_5^* & A_6^* \end{pmatrix}^T$,

$$S_H = \begin{pmatrix} \rho UBK_h\dot{h}_1 & \rho UB^2K_\alpha\dot{\alpha}_1 & \rho U^2BK_\alpha^2\alpha_1 & \rho U^2K_h^2h_1 & \rho UBK_p\dot{p}_1 & \rho U^2K_p^2p_1 \\ \rho UBK_h\dot{h}_2 & \rho UB^2K_\alpha\dot{\alpha}_2 & \rho U^2BK_\alpha^2\alpha_2 & \rho U^2K_h^2h_2 & \rho UBK_p\dot{p}_2 & \rho U^2K_p^2p_2 \\ \vdots & \vdots & \vdots & \vdots & \vdots & \vdots \\ \rho UBK_h\dot{h}_n & \rho UB^2K_\alpha\dot{\alpha}_n & \rho U^2BK_\alpha^2\alpha_n & \rho U^2K_h^2h_n & \rho UBK_p\dot{p}_n & \rho U^2K_p^2p_n \end{pmatrix},$$

$$S_P = \begin{pmatrix} \rho UBK_p\dot{p}_1 & \rho UB^2K_\alpha\dot{\alpha}_1 & \rho U^2BK_\alpha^2\alpha_1 & \rho U^2K_p^2p_1 & \rho UBK_h\dot{h}_1 & \rho U^2K_h^2h_1 \\ \rho UBK_p\dot{p}_2 & \rho UB^2K_\alpha\dot{\alpha}_2 & \rho U^2BK_\alpha^2\alpha_2 & \rho U^2K_p^2p_2 & \rho UBK_h\dot{h}_2 & \rho U^2K_h^2h_2 \\ \vdots & \vdots & \vdots & \vdots & \vdots & \vdots \\ \rho UBK_p\dot{p}_n & \rho UB^2K_\alpha\dot{\alpha}_n & \rho U^2BK_\alpha^2\alpha_n & \rho U^2K_p^2p_n & \rho UBK_h\dot{h}_n & \rho U^2K_h^2h_n \end{pmatrix},$$

$$S_A = \begin{pmatrix} \rho UB^2K_h\dot{h}_1 & \rho UB^3K_\alpha\dot{\alpha}_1 & \rho U^2B^2K_\alpha^2\alpha_1 & \rho U^2BK_h^2h_1 & \rho UB^2K_p\dot{p}_1 & \rho U^2BK_p^2p_1 \\ \rho UB^2K_h\dot{h}_2 & \rho UB^3K_\alpha\dot{\alpha}_2 & \rho U^2B^2K_\alpha^2\alpha_2 & \rho U^2BK_h^2h_2 & \rho UB^2K_p\dot{p}_2 & \rho U^2BK_p^2p_2 \\ \vdots & \vdots & \vdots & \vdots & \vdots & \vdots \\ \rho UB^2K_h\dot{h}_n & \rho UB^3K_\alpha\dot{\alpha}_n & \rho U^2B^2K_\alpha^2\alpha_n & \rho U^2BK_h^2h_n & \rho UB^2K_p\dot{p}_n & \rho U^2BK_p^2p_n \end{pmatrix}.$$

If the self-excited lift force, drag force, and torsional moment, i.e., F_L, F_D, M_T are obtained from experimentally measured or numerically simulated time-varying force/moment histories, the values of X_H, X_P and X_A can be estimated using

$$X_H = \left(S_H^T S_H\right)^{-1} S_H^T F_L \tag{3a}$$

$$X_P = \left(S_P^T S_P\right)^{-1} S_P^T F_D \tag{3b}$$

$$X_A = \left(S_A^T S_A\right)^{-1} S_A^T M_T \tag{3c}$$

For the 3-DOF coupled case, all 18 flutter derivatives can be simultaneously extracted using this standard pseudo-inverse matrix approach.

3. Discussions on some details

3.1 Requirement for different coupled vibration frequencies

Different frequencies are necessary in coupled forced vibration method. If $\omega_h = \omega_\alpha = \omega_p$, then the six column vectors in S_H, S_P, and S_A in Eq. (2) are linearly dependent, respectively. Thus, $\left(S_H^T S_H\right)^{-1}$, $\left(S_P^T S_P\right)^{-1}$, and $\left(S_A^T S_A\right)^{-1}$ in Eq. (3) are ill-conditioned matrices, and X_H, X_P and X_A cannot be extracted from Eq. (3). Although Guo (2006) and Niu *et al.* (2007) developed the coupled forced vibration setups, and the criterion of $\omega_h \neq \omega_\alpha \neq \omega_p$ was used in their tests, the reason for this criterion was not publicly mentioned in their studies. Therefore, this study contributes an instruction that in coupled forced vibration method, whether experimental or numerical, the different frequencies of three coupled modes, i.e., $\omega_h \neq \omega_\alpha \neq \omega_p$ are indispensible requirements.

3.2 Various components of force and moment

Due to vibrate in smooth flows, the aerodynamic buffeting components are negligible and omitted herein for brevity. For numerical simulations and or experimental tests, h_i, $\dot{h}_i$, p_i, $\dot{p}_i$, α_i, $\dot{\alpha}_i$ can be accurately prescribed and determined. So, the accuracies of S_H, S_P, and S_A in Eq. (3) can be easily ensured. Thus, the accurate determination of F_L, F_D, M_T is one key factor for quantifying flutter derivatives. The numerically simulated results include the aerostatic components and aeroelastic components, and additional inertia force and moment components are also included in the experimentally collected data. Seemingly, it is very easy to obtain F_L, F_D, M_T for both experiments and simulations. Actually, many complexities are incorporated and the issues of aerostatic components and inertia force and moment components require to be clarified. Then, some new insights and improved understandings will be achieved.

4. Influence of aerostatic component on flutter derivatives

Taking the aeroelastic lift force as an example, the components contributed by $H_{1\sim6}^*$ can be represented by

$$S = [s_1\ s_2\ s_3\ s_4\ s_5\ s_6] \tag{4}$$

where, $S \in R^{n\times6}$, $s_i = A_i \sin(\omega_i t + \phi_i)$ are sinusoidal waves, $i = 1, 2, \cdots, 6$.

Assuming $(S^T S)^{-1} = \begin{bmatrix} b_{11} & \cdots & b_{16} \\ \vdots & \ddots & \vdots \\ b_{61} & \cdots & b_{66} \end{bmatrix}$, and, $(S^T S)^{-1} \in R^{6\times6}$. Then,

$$A=(S^TS)^{-1}S^T=\begin{bmatrix} b_{11} & \cdots & b_{16} \\ \vdots & \ddots & \vdots \\ b_{61} & \cdots & b_{66} \end{bmatrix}\begin{bmatrix} s_1^T \\ \vdots \\ s_6^T \end{bmatrix}=\begin{bmatrix} \sum_{i=1}^{6} b_{1i}s_i^T \\ \vdots \\ \sum_{i=1}^{6} b_{6i}s_i^T \end{bmatrix} \tag{5}$$

where, $A\in R^{6\times n}$, and each component of matrix A can be expressed as the summation of six sinusoidal waves with three different frequencies, and six different amplitudes and phases.

Consider the aerostatic force to be a constant and denoted as *C*, the total wind action force (buffeting response is considered to be negligible and excluded) can be expressed as

$$T_L=C+F_L=C+\begin{pmatrix} F_{L1} & F_{L2} & \cdots & F_{Ln} \end{pmatrix}^T \tag{6}$$

If $t\to\infty$ or $t=nT$, $T=lcm(2\pi/\omega_h, 2\pi/\omega_p, 2\pi/\omega_\alpha)$, where T is the least common multiple of three modal periods. For the forced (numerical and experimental) vibrations, the frequencies can be known exactly. However, they are difficult or impossible to be accurately determined for the free vibrations. Under such conditions, due to the orthogonality of the simple harmonics, then

$$\left(S_H^TS_H\right)^{-1}S_H^TC=0 \tag{7}$$

Subsequently

$$\left(S_H^TS_H\right)^{-1}S_H^TT_L=\left(S_H^TS_H\right)^{-1}S_H^T(C+F_L)=\left(S_H^TS_H\right)^{-1}S_H^TF_L=X_H \tag{8}$$

In other words, X_H is independent of the constant parameter C. Similarly, X_P, X_A are also independent of arbitrary constants. It means that any constant force have no influence on flutter derivatives with the conditions of $t\to\infty$ or $t=nT$. Actually, it is impossible to make $t\to\infty$, so $t=nT$ is a practical solution. It provides a convincing proof that if $t=nT$, the average component is unnecessary to be subtracted from the total force to extract flutter derivatives. Although it seems to be meaningless from the practical viewpoint, it is beneficial for better understanding this issue. Moreover, more or less errors are unavoidable for the average aerostatic force component. Even this component result is completely wrong, it has no influence on the extraction results. This viewpoint is initially presented in this study, and it is also an encouraging message for researchers. They need not worry about the influence of inaccurate aerostatic force on flutter derivative. Bear in mind, $t=nT$ is the indispensible requirement.

5. Influence of inertia force and moment on flutter derivatives

The inertia force and moment are included in experimental tests while not concerned in numerical simulations. Consider a deck model with mass and mass of moment of m and I in wind tunnel tests, if it vibrates in coupled modes as $h(t)=h_0\sin(\omega_h t+\varphi_h)$, $p(t)=p_0\sin(\omega_p t+\varphi_p)$, $\alpha(t)=\alpha_0\sin(\omega_\alpha t+\varphi_\alpha)$, respectively. The inertia force and moment can be respectively denoted as

$$F_{L-I}(t) = -mh_0\omega_h{}^2 \sin(\omega_h t + \varphi_h) \tag{9a}$$

$$F_{D-I}(t) = -mp_0\omega_p{}^2 \sin(\omega_p t + \varphi_p) \tag{9b}$$

$$M_{T-I}(t) = -I\alpha_0\omega_\alpha{}^2 \sin(\omega_\alpha t + \varphi_\alpha) \tag{9c}$$

Many efforts have been attempted to reduce m and I for minimizing the inertia force and moment, by which the accuracy of aeroelastic components can be improved. According to Eq. (1), the vertical, lateral, and torsional inertial force or moment directions have the same directions with displacements.

$$\rho U^2 B K_h{}^2 H_4^* \frac{h}{B} = F_{L-I} = -m\omega_h{}^2 h \tag{10a}$$

$$\rho U^2 B K_p{}^2 P_4^* \frac{P}{B} = F_{D-I} = -m\omega_p{}^2 p \tag{10b}$$

$$\rho U^2 B^2 K_\alpha{}^2 A_3^* \alpha = M_{T-I} = -I\omega_\alpha{}^2 \alpha \tag{10c}$$

It means that only H_4^*, P_4^*, and A_3^* are related to inertial force or moment. In other words, if $t = nT$, the inertia force and moment component is unnecessary to be accurately quantified to extract other 15 flutter derivatives. The modifications of H_4^*, P_4^*, and A_3^* due to inertial force or moment can be easily written as

$$\Delta H_4^* = -\frac{m}{\rho B^2} \tag{11a}$$

$$\Delta P_4^* = -\frac{m}{\rho B^2} \tag{11b}$$

$$\Delta A_3^* = -\frac{I}{\rho B^4} \tag{14c}$$

In summary, if the signal length is sufficiently long or appropriate (i.e., $t \to \infty$ or $t = nT$), the aerostatic components and inertia force and moment components have no influences on flutter derivatives. In addition, the criterion of $t = nT$ ($n \geq 5$) for signal interval selection is recommended.

6. Numerical example

6.1 Associated parameters

The 3-DOF Sutong Bridge (a cable-stayed bridge with a main span length of 1088 m, China) deck model (Xu *et al*. 2012) is used to investigate the imperfections of the currently prevailing framework for flutter derivatives extraction. Taking the aeroelastic lift force and the

corresponding $H_{1\sim6}^{*}$ as an example, four cases are included to explore the influences of signal length, amplitude, and frequency on identification results, and the associated parameters are listed in Table 1. For the concerned four cases, the deck model width (B=1 m) and wind velocity (U=10 m/s) are assumed to quantify flutter derivatives with different frequencies. It needs to be mentioned that the initial phase angles can be randomly set, and they are all set as zeros herein for convenient comparison and without loss of generality. Analogously, similar simulation and analysis can be performed for $A_{1\sim6}^{*}$ and $P_{1\sim6}^{*}$, which are omitted herein for the sake of length.

6.2 Average of self-excited force

Taking the lift force as an example, allowing for the aerostatic component (denoted as C), the numerically simulated forces can be expressed as $F_T(t)=F_L(t)+C$. The series of $F_T(t)-m_{F_T(t)}$ are usually treated as the aeroelastic component $F_L(t)$, and $m_{F_T(t)}$ is the average of $F_T(t)$. It is noted that $F_T(t)-m_{F_T(t)}=F_L(t)-m_{F_L(t)}$, and $m_{F_L(t)}$ is the average of $F_L(t)$. Theoretically, if nonlinear effects are negligible, the average of aeroelastic lift force should be zero. Practically, the calculated $m_{F_L(t)}$ varies with t. It indicates that $F_L(t)$ cannot be accurately calculated by $F_T(t)-m_{F_T(t)}$ or $F_L(t)-m_{F_L(t)}$ for most cases, and it is appropriate only under the condition of $t=nT$. Fig. 2 shows the curves of $m_{F_L(t)}$ for four cases.

Some key findings from these results are as follows: For each case, the corresponding t for $m_{F_L(t)}$=0 are different. For Cases1-3, if $t=nT$ ($n=1,2,3,...$, $T=4$ s), $m_{F_L(t)}$=0, which are marked in Fig. 2. For Case 4, due to $T\neq4$ s, so $m_{F_L(4)}\neq0$, $m_{F_L(8)}\neq0$. Due to $T=10$ s, and $m_{F_L(10)}=0$. Besides $t=nT$, $m_{F_L(t)}$ for other time durations may be zero.

6.3 Flutter derivatives

If $F_L(t)$ are calculated by $F_T(t)-m_{F_T(t)}$, flutter derivatives can be subsequently extracted according to Eq. (3(a)). It is widely accepted that the identification results are theoretically independent of signal length. For Case 1, the curves of flutter derivative deviations from their initial goals (listed in Table 1) versus time durations are shown in Fig. 3.

Table 1 Related parameters for different cases

Case	h_0 (m)	p_0 (m)	α_0 (º)	ω_h (rad/s)	ω_p (rad/s)	ω_α (rad/s)	H_1^*	H_2^*	H_3^*	H_4^*	H_5^*	H_6^*
1	0.02	0.02	2	2.0π	1.5π	2.5π	-3.2	-0.3	-4	-0.6	-0.1	-0.1
2	**0.002**	0.02	2	2.0π	1.5π	2.5π	-3.2	-0.3	-4	-0.6	-0.1	-0.1
3	0.02	0.02	2	$\mathbf{4.0}\pi$	1.5π	2.5π	**-1.5**	-0.3	-4	**-0.4**	-0.1	-0.1
4	0.02	0.02	2	2.0π	$\mathbf{1.8}\pi$	$\mathbf{2.2}\pi$	-3.2	**-0.4**	**-5.5**	-0.6	**-0.12**	**0.0**

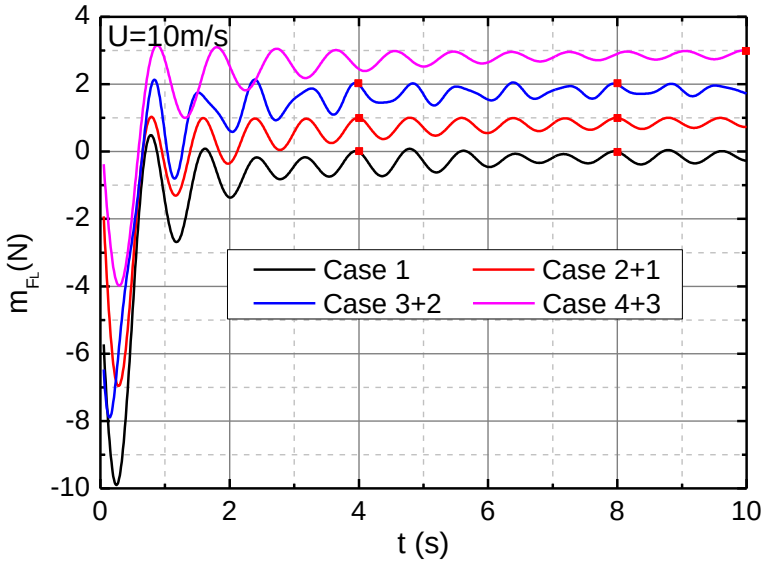

Fig. 2 Variations of average aeroelastic force with different time durations

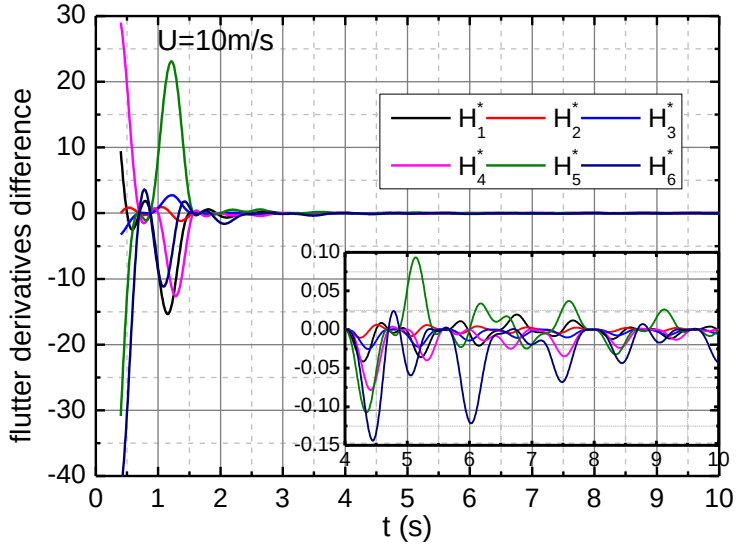

Fig. 3 Flutter derivatives difference for Case1 with different time durations

Some key findings from these results are as follows:

(1) Significant deviations can be seen when $t < 2$. In other words, if the signal is too short, the identified results may be completely wrong.

(2) The deviations appear to be negligible when $t > 4$. Looking at the zoomed figure closely, deviations are noticeable for $H^*_{5,6}$. It is therefore important to ensure sufficiently long data to acquire acceptable accuracies.

(3) Due to T =4 s, when t =4, 8 s, the deviations for all flutter derivatives are zeros.

Similar to Case 1, if $t<4$, the deviations are remarkable for the other three cases. Therefore, for short time duration, the deficiency of $F_T(t)-m_{F_T(t)}$ for customarily calculating aeroelastic force is fully demonstrated. The signal length $t=nT$ is strongly recommended for parameter identification. The flutter derivatives deviations for all four cases are shown in Fig. 4 for comparison.

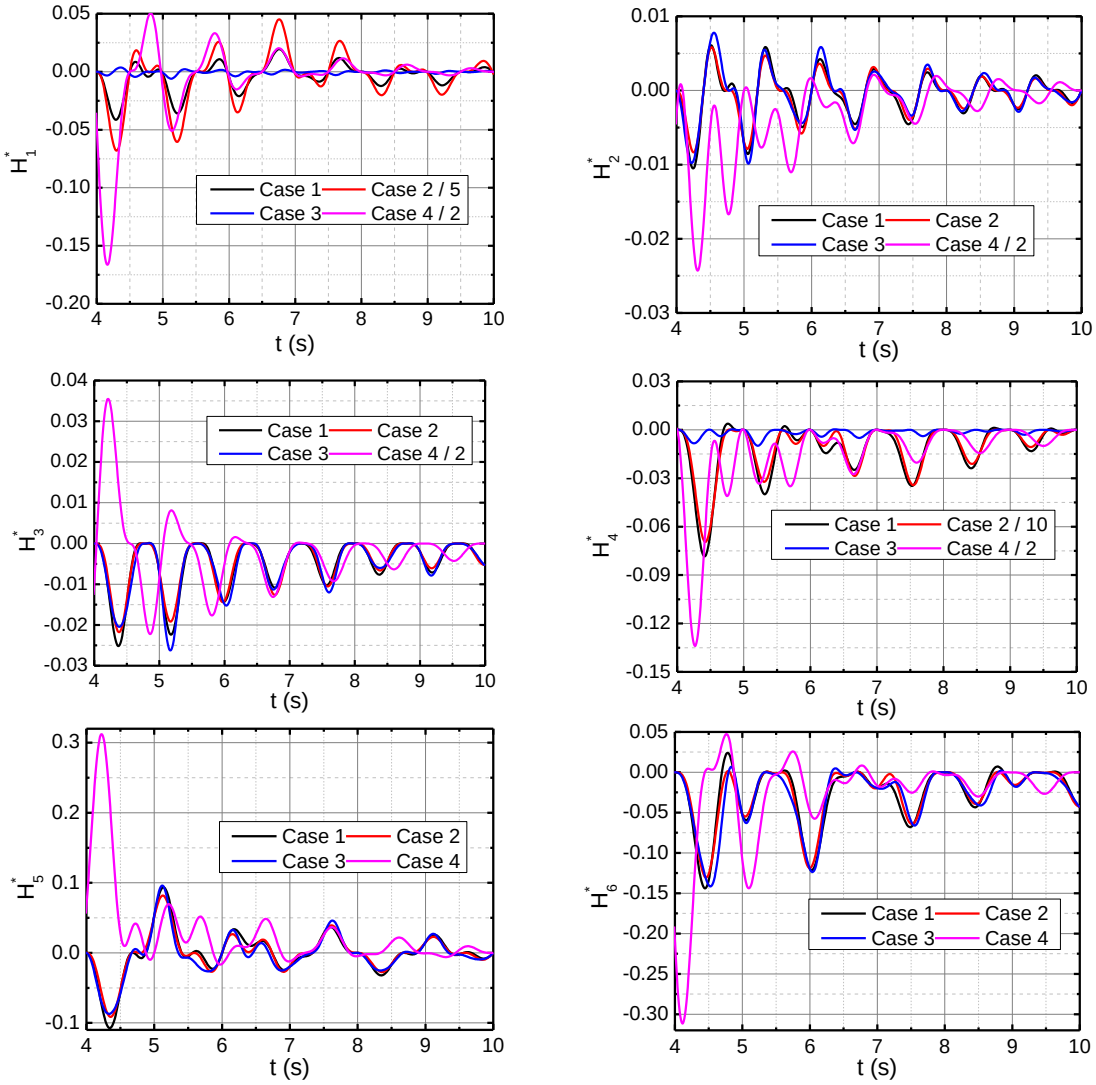

Fig. 4 Flutter derivatives difference for four cases with different time durations

Influence of amplitude. Compared to Case 2, Case 1 shows better accuracy for H_1^* and H_4^*. It can be concluded that a lower amplitude decreases its component weight in self-excited force, and the corresponding flutter derivatives accuracies decline. Therefore, very low amplitudes (e.g., amplitude <0.005 m) is unacceptable in practice. On the other hand, large amplitudes cause aeroelastic nonlinearity (Scanlan 1997 and Noda *et al*. 2003), which must also be avoided.

Influence of frequency ratio. Comparing Case 4 to Case 1, if three frequencies are getting closer, the $H_{1\sim4}^*$ accuracies will subsequently decline. The lower torsional frequency reduces the accuracies of $H_{2,3}^*$. Matsumoto *et al*. (1993) also noticed the flutter derivatives are independent on modal coupling in forced vibration tests.

For the aforementioned cases, not any noise is included, i.e., the signals are ideal. The extraction results are closely related to signal length, amplitude, and frequency ratio of components. For experimental tests, perfect harmonic oscillation cannot be ensured and the instruments are also imperfect more or less. So, various noises are included in the collected signals. It can be anticipated that more obvious errors will be unavoidable. Even $t = nT$, the noises also contaminate the results. However, if the noises are white and *t* is sufficiently long, the average of noise tends to be zero. The influence of noise cannot be completely eliminated. Therefore, empirical or even arbitrary selection of t may result in unacceptable errors for short time durations of experimental data. Frankly, it is easily accepted that high accuracy can be achieved by using long time duration of signal. This study demonstrates the necessity of this criterion and reveals the seriousness of arbitrary selection of t, especially for short time.

For different cross sections with different reduced velocities, the influences may be different more or less. The similar phenomena can be observed, and no extra cases are included for the sake of length. In addition, it is admitted that cross-influences among different flutter derivatives exist, and single-parameter analysis has some imperfections. One major aim is to sound the alarm for better understanding this issue, and further to achieve high-accuracy extraction results. Based on the identified flutter derivatives, the multiple-mode flutter analyses can be subsequently conducted, which have been extensively addressed (Yang *et al*. 2007, Hua *et al.* 2008, Matsumoto *et al.* 2010).

7. Bridge deck case study

7.1 Related parameters

The Sunshine Skyway Bridge (a cable-stayed bridge with a main span length of 364 m, America) has a bluff box girder section (Bartoli *et al*. 2009), which is slightly simplified and proportionally portrayed in Fig. 5.

The aerodynamic derivatives were experimentally identified in wind tunnel by Mannini and Bartoli (2008), and the unsteady aerodynamic properties were numerically investigated using RANS model by Mannini *et al*. (2010). The 3-DOF coupled forced numerical technique is used to acquire the wind-induced loading responses, and the related parameters in numerical simulation are listed in Table 2. The computation step is 0.002 s, and the selected time interval is [5.40 s, 11.88 s], in which the vertical, lateral, and torsional motions completed 6, 4, and 8 periods, respectively. The accuracy and efficacy of the 3-DOF coupled forced numerical technique were fully validated in another study (Xu *et al*. 2014).

Table 2 Numerical simulation parameters

B(m)	U(m/s)	T (s)	h_0 (m)	p_0 (m)	α_0 (º)
0.45	5	3.24	0.005	0.005	2
ω_h (rad/s)	ω_p (rad/s)	ω_α (rad/s)	φ_h (rad)	φ_p (rad)	φ_α (rad)
1.8519π	1.2346π	2.4691π	0	0	0

7.2 Average of self-excitated force and fitting error

The curves of $F_L(t)$ and $m_{F_L(t)}$ versus t are shown in Fig. 6. The time interval of [5.40 s, 8.64 s] is also an appropriate selection for signal length. Moreover, $F_L(t)$ in intervals of [5.40 s, 8.64 s] and [8.64 s, 11.88 s] are almost identical. The drag force and torsional moment can also be synchronously achieved, but is beyond the scope of this paper for brevity.

If nonlinear aerodynamic effects can be neglected, the rational aerostatic response is calculated to be about 0.2904 N with $t = 2T = 6.48$ s. If t=2, 4, and 6.48 s, $m_{F_L(2)} = 0.3685$, $m_{F_L(4)} = 0.2870$, $m_{F_L(6.48)} = 0.2904$ N, respectively. In Fig. 6, due to the initial time is 5.40 s, the time instants of 8.64 s and 11.88 s correspond to T, $2T$, respectively. Therefore, the aerostatic average from initial time to these two time instants is 0.2904 N. Substituting $F_L(t) - m_{F_L(t)}$ into Eq. 3(a), the flutter derivatives can be extracted. Then the fitting lift aeroelastic force $F'_L(t)$ can be directly calculated via Eq. (3(a)) using motion displacements, velocities, and the just extracted flutter derivatives. The aerostatic lift force (0.2904 N) is added to $F'_L(t)$, and the difference between $F_L(t)$ and $F'_L(t) + 0.2904$, i.e., the fitting errors of $F_L(t) - F'_L(t) - 0.2904$ are also shown in Fig. 6. Some key findings from these results are as follows: Noticeable periodical fitting errors are detected. Apparently, the fitting errors are not random noises. Further, even though the nominal aerostatic force (0.2904 N) is subtracted from the originally calculated lift force, the aeroelastic lift force distribution is not symmetrical to the zero axis, which is induced by the asymmetrical bluff section and high-order components. For example, the maximum and minimum forces are approximately equal to 1.3 N and -1.5 N, respectively. This indicates that the absolute values of the maximum and minimum are not identical. Therefore, it can be concluded that the nonlinear aeroelastic component plays the key role. For the time durations of 4 s and 6.48 s, the corresponding fitting errors are almost identical. However, the fitting error for the case of 2 s is slightly different.

7.3 Flutter derivatives

The aerostatic force is closely related to attack angle, i.e., the aerostatic force cannot be constant during torsional vibration. For an example, for a thin flat plate, the aerostatic drag force may be considered as zero for small torsional vibration. The average drag force linearly increases with torsional amplitude within the stall angle region. For another example, for an asymmetric section, the average lift force and torsional moment in one oscillation period are usually not equal to the aerostatic force at the zero angle of incidence.

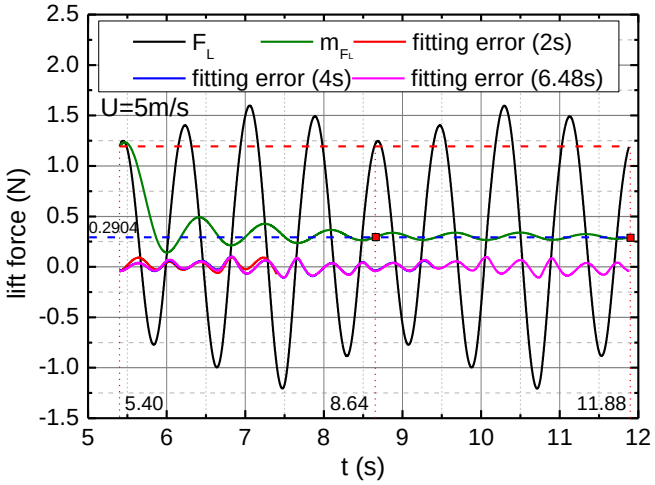

Fig. 6 Variations of lift force with different time durations

It is challenging to accurately quantify the angle-varying force, and therefore has to be simplified to an approximate constant. The aerostatic force is independent of signal length. However, the average response (customarily regarded as the nominal aerostatic component) relies heavily on the signal length, especially for short signals. Two cases are analyzed in this study: Case 1 adopts the traditional approach of using the directly calculated average values which vary with signal length. Case 2 uniformly uses the reasonable value of 0.2904 N, -0.3373 N·m, 0.6737 N for aerostatic lift force, torsional moment, and drag force for all signal lengths.

Fig. 7 shows the extracted flutter derivatives for two cases. Similar to the results shown in Fig. 3, when t is too short, the identified results may be completely wrong. Therefore, only the results for $t > 2.6$ s are provided in Fig. 7. Some key findings from these results are as follows:

(1) When $8 \leq t \leq 11.88$ s, obvious fluctuations are observed, especially for $H_{4\sim6}^{*}$. The major origin should be the relative lower amplitude for the corresponding aeroelastic force components.

(2) The results for Cases 1 and 2 are different, and the differences are more remarkable for shorter t. The aerostatic force for Case 2 is more rational, and the corresponding fluctuations of flutter derivatives are relatively smooth. When $t = 8.64, 11.88$ s, the aerostatic average is 0.2904 N, and the two sets of flutter derivatives are identical.

(3) Even though when $t >$ 11 s, $H_{4\sim6}^{*}$ cannot be accurately determined. Therefore, the accuracy of $H_{4\sim6}^{*}$ cannot be ensured without appropriate selection of signal length. Meanwhile, this issue has ever tortured many researchers and warrants further research.

The feature of flutter derivatives fluctuation with time alerts us the significance of appropriate selection of signal length. Results from this example case study demonstrate that if the signal is sufficiently long, the averages of calculated and/or measured forces have negligible influence on flutter derivatives, which was just proved in the foregoing context. The aeroelastic lift forces in time interval of [5.40 s, 11.88 s] are duplicated fifteen times and extended to the interval of [5.40 s, 109.08 s]. Then the newly generated lift force history (Actually, it can also be achieved by longer time of testing or numerical simulation.) is regarded as the original aeroelastic force signal. Substituting this signal series (note that the average is not eliminated) into Eq. (3(a)), the flutter derivatives can be easily obtained, which are provided in Fig. 10.

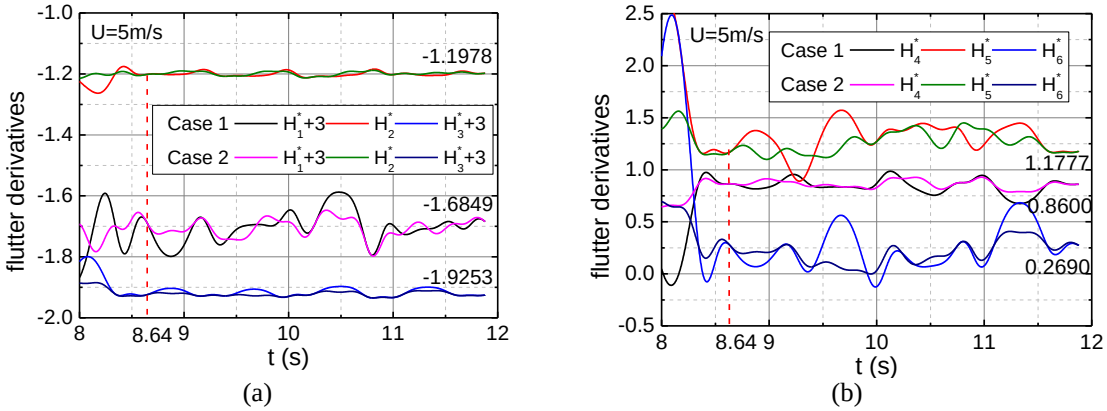

Fig. 7 Flutter derivatives with different time durations: (a) $H^*_{1\sim3}$; (b) $H^*_{4\sim6}$

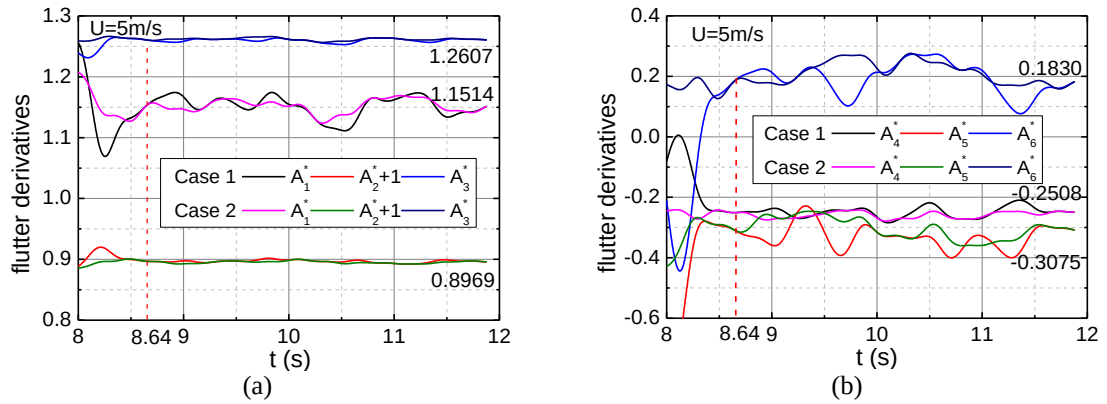

Fig. 8 Flutter derivatives with different time durations: (a) $A^*_{1\sim3}$; (b) $A^*_{4\sim6}$

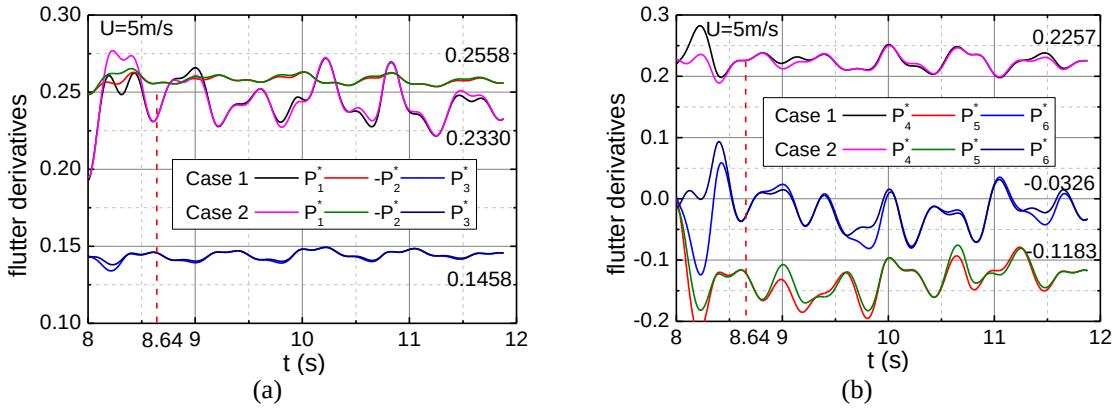

Fig. 9 Flutter derivatives with different time durations: (a) $P^*_{1\sim3}$; (b) $P^*_{4\sim6}$

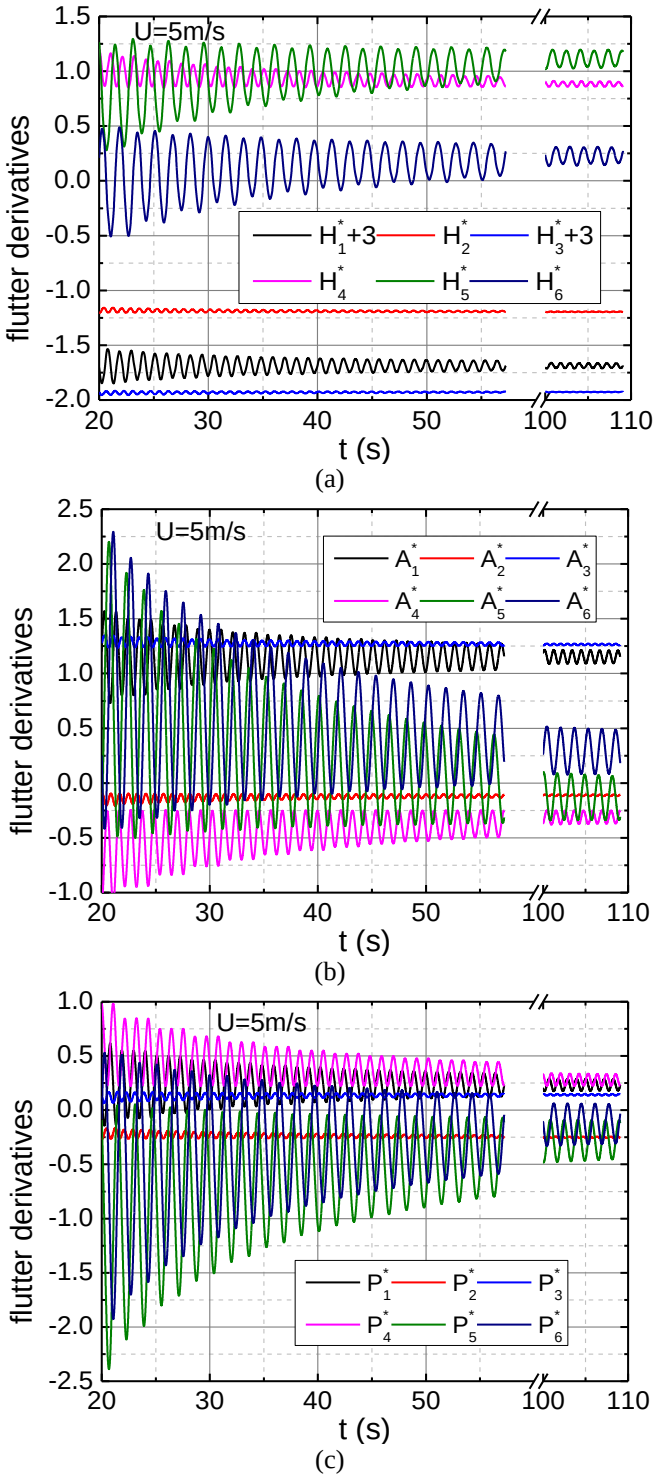

Fig. 10 Flutter derivatives with different time durations: (a) $H_{1\sim6}^*$; (b) $A_{1\sim6}^*$; (a) $P_{1\sim6}^*$

Some key findings from these results are as follows:

(1) With increasing signal length, the results tend to converge. This means the values of $\left(S_H^T S_H\right)^{-1} S_H^T$ decrease with signal length.

(2) The results of $H_{4\sim6}^*$ are relatively more sensitive to signal length. The corresponding aeroelastic lift force components are negligible, and the corresponding elements in $\left(S_H^T S_H\right)^{-1} S_H^T$ are more difficult to be accurately determined.

(3) Satisfactory accuracy for $H_{2\sim3}^*$ can be achieved when $t > 20\,\text{s}$, and $t > 40\,\text{s}$ for H_1^*, and $t > 60\,\text{s}$ for H_4^*. However, even when $t > 100\,\text{s}$, $H_{5\sim6}^*$ show noticeable fluctuation, which attribute to their intrinsic properties.

The above analyses can also be employed to $A_{1\sim6}^*$ and $P_{1\sim6}^*$, and to other bridge deck cases, similar phenomena can be observed, which are omitted herein for the sake of length.

8. Conclusions

For identifying bridge deck flutter derivatives with coupled forced vibration method, the issues related to modal frequencies adoption, signal length selection, influences of aerostatic force component and inertia force and moment on flutter derivatives identification are analyzed using theoretical simulations and practical considerations. The main findings and conclusions from this study are summarized as follows.

(1) To extract flutter derivatives of a bridge deck using a 3-DOF coupled forced vibration method, three different frequencies of three vibration modes are required, and the mathematical proof is offered. It contributes an instructional criterion for future investigations on flutter derivatives identification using experimentally and/or numerically coupled forced vibration methods.

(2) If $t = nT$ (T is the least common multiple of coupled modal periods), the aerostatic components, inertia force and moment components are theoretically proved to have no influences on flutter derivatives. They are also demonstrated by two bridge deck examples. So, even the aerostatic components, inertia force and moment components are not accurately determined, satisfactory accuracy can be achieved for flutter derivatives. If the signal length *t* is too short, the wrong results may be obtained. Therefore, the signal length $t = nT$ ($n \geq 5$) is strongly recommended for flutter derivatives identification.

(3) Practically, it is demonstrated that the identification accuracies of flutter derivatives increase with the corresponding modal amplitude and frequency. In addition, for the coupled forced vibration method, some aeroelastic force components may be comparatively negligible, and it is challenging to accurately quantify the corresponding flutter derivatives (e.g., $H_{4\sim6}^*$).

Acknowledgments

The research is financially supported by the National Science Foundation of China (No. 51178086, 51478087), they are gratefully acknowledged.

References

Bartoli, G., Contri, S., Mannini, C. and Righi, M. (2009), "Toward an improvement in the identification of bridge deck flutter derivatives", *J. Eng. Mech. - ASCE*, **135**(8), 771-785.

Chen, Z., Yu, X., Yang, G. and Spencer Jr, B. (2005), "Wind-induced self-excited loads on bridges", *J. Struct. Eng. - ASCE*, **131**(12), 1783-1793.

Diana, G., Resta, F., Zasso, A., Belloli, M. and Rocchi, D. (2004), "Forced motion and free motion aeroelastic tests on a new concept dynamometric section model of the Messina suspension bridge", *J. Wind Eng. Ind. Aerod.*, **92**(6), 441-462.

Falco, M., Curami, A. and Zasso, A. (1992), "Nonlinear effects in sectional model aeroelastic parameters identification", *J. Wind Eng. Ind. Aerod.*, **42**(1), 1321-1332.

Guo, Z. (2006), *Three degree-of-freedom forced vibration method for identification of aerodynamic derivatives of bridge decks*, Ph.D. dissertaion, Tongji University, China.

Hua, X. and Chen, Z. (2008), "Full-order and multimode flutter analysis using ANSYS", *Finite Elem. Anal. Des.*, **44**(9), 537-551.

Li, Q. (1995), "Measuring flutter derivatives for bridge sectional models in water channel", *J. Eng. Mech. - ASCE*, **121**(1), 90-101.

Mannini, C. and Bartoli, G. (2008), "Investigation on the dependence of bridge deck flutter derivatives on steady angle of attack", *Proceedings of the BBAAVI Int. Colloquium on Bluff Bodies Aerodynamics and Applications*, Milano, Italy.

Mannini, C., Šoda, A., Voß, R. and Schewe, G. (2010), "Unsteady RANS simulations of flow around a bridge section", *J. Wind Eng. Ind. Aerod.*, **98**(12), 742-753.

Matsumoto, M., Matsumiya, H., Fujiwara, S. and Ito, Y. (2010), "New consideration on flutter properties based on step-by-step analysis", *J. Wind Eng. Ind. Aerod.*, **98**(8), 429-437.

Matsumoto, M., Shiraishi, N., Shirato, H., Shigetaka, K. and Niihara, Y. (1993), "Aerodynamic derivatives of coupled/hybrid flutter of fundamental structural sections", *J. Wind Eng. Ind. Aerod.*, **49**(1), 575-584.

Niu, H., Chen, Z., Liu, M., Han, Y. and Hua, X. (2007), "Development of the 3-DOF forced vibration device to measure the aerodynamic forces on section models", *Proceedings of the 12th International Conference on Wind Engineering*, Cairns, Australia.

Noda, M., Utsunomiya, H., Nagao, F., Kanda, M. and Shiraishi, N. (2003), "Effects of oscillation amplitude on aerodynamic derivatives", *J. Wind Eng. Ind. Aerod.*, **91**(1), 101-111.

Scanlan, R.H. (1997), "Amplitude and turbulence effects on bridge flutter derivatives", *J. Struct. Eng. - ASCE*, **123**(2), 232-236.

Shirai, S. and Ueda, T. (2003), "Aerodynamic simulation by CFD on flat box girder of super-long-span suspension bridge", *J. Wind Eng. Ind. Aerod.*, **91**(1), 279-290.

Singh, L., Jones, N., Scanlan, R. and Lorendeaux, O. (1996), "Identification of lateral flutter derivatives of bridge decks", *J. Wind Eng. Ind. Aerod.*, **60**, 81-89.

Sun, D., Owen, J. and Wright, N. (2009), "Application of the k–ω turbulence model for a wind-induced vibration study of 2D bluff bodies", *J. Wind Eng. Ind. Aerod.*, **97**(2), 77-87.

Ukeguchi, N., Sakata, H. and Nishitani, H. (1966), "An investigation of aeroelastic instability of suspension bridges", *Proceedings of the Int. Symposium on Suspension Bridges*, Lisbon.

Vairo, G. (2003), "A numerical model for wind loads simulation on long-span bridges", *Simul. Model. Pract. Th.*, **11**(5), 315-351.

Walther, J.H. and Larsen, A. (1997), "Two dimensional discrete vortex method for application to bluff body aerodynamics", *J. Wind Eng. Ind. Aerod.*, **67**, 183-193.

Xu, F., Chen, X., Cai , C. and Chen, A. (2012), "Determination of 18 flutter derivatives of bridge decks by an improved stochastic search algorithm", *J. Struct. Eng. -ASCE*, **17**(4), 576-588.

Xu, F., Ying, X. and Zhang Z. (2014), "A 3-DOF coupled numerical technique for extracting 18 aerodynamic derivatives of bridge decks", *J. Struct. Eng. - ASCE*, 10.1061/(ASCE)ST. 1943-541X. 0001009.

Yang, Y., Ge, Y. and Xiang, H. (2007), "Investigation on flutter mechanism of long-span bridges with 2d-3DOF method", *Wind Struct.*, **10**(5), 421-436.
Zhou, Z. and Ma, R. (2010), "Numerical simulation study of the Reynolds number effect on two bridge decks based on the deterministic vortex method", *Wind Struct.*, **13**(4), 347-362.

CC